Available online at www.sciencedirect.com

ScienceDirect

Advances in Space Research 67 (2021) 2534–2543

ADVANCES IN SPACE RESEARCH (a COSPAR publication)

www.elsevier.com/locate/asr

Modelling of protons spectra encountered in space using medical accelerator and its microdosimetric characterization

S. Peracchi [a,*], B. James [a], S. Psoroulas [b], M. Grossmann [b], D. Meer [b], D. Bolst [a], Z. Pastuovic [c], J. Vohradsky [a], S. Guatelli [a], D.A. Prokopovich [a,c], M. Petasecca [a], M. L.F. Lerch [a], M. Povoli [d], A. Kok [d], M. Jackson [a,e], A.B. Rosenfeld [a,*], L.T. Tran [a]

[a] Centre of Medical and Radiation Physics, University of Wollongong, Australia
[b] Centre for Proton Therapy, Paul Scherrer Institute, Switzerland
[c] Australian Nuclear Science and Technology Organization, Australia
[d] SINTEF MiNaLab, Norway
[e] University of New South Wales, Australia

Received 16 September 2020; received in revised form 27 December 2020; accepted 21 January 2021
Available online 11 February 2021

Abstract

Radiation environments in space are mainly composed of protons coming from the Galactic Cosmic Rays (GCRs) pervading the universe, the Solar Particle Events (SPEs) resulting from solar flares and coronal mass ejections, and the two Van Allen Belts surrounding the Earth due to the presence of the geomagnetic field trapping charged particles. Their wide spectra of energies up to hundreds of GeV imply diverse radiobiological effects to astronauts and radiation damage to electronics in the spacecraft. Even if lower in abundance, heavy ions such as He, C, O, Si, Fe are present in space and constitute an even bigger hazard due to their high penetrability and high linear energy transfer (LET). Most irradiation facilities available for research and testing worldwide provide usually only monoenergetic beams of high-energy protons or other heavier particles limiting studies of radiobiological effects and effects on electronics to a set of discrete energies.

This paper introduces a procedure where a proton fluence spectra of interest for space radiation protection, previously generated by Monte Carlo simulations was delivered using a clinical proton therapy accelerator. Particularly, it reports the first results of modelling a proton radiation field in space in the energy range from 70 to 230 MeV during a single experimental session by programming a treatment planning system (TPS) to deliver required proton irradiation energies. Moreover, the angular distribution of the proton irradiation field has been varied to reproduce the isotropic exposure experienced by humans in space. The obtained proton radiation field was characterized using a 3D sensitive volume SOI microdosimeter developed by the Centre for Medical Radiation Physics (CMRP), University of Wollongong, Australia.

Keywords: SOI microdosimeter; ISS; GCR; SPE; Protons; Fluence

1. Introduction

Humans involved in space exploration are constantly being exposed to radiation. The main portion of radiation is related to high-energy protons originating from different

* Corresponding authors at: Centre of Medical and Radiation Physics, University of Wollongong, Australia.
E-mail addresses: sp009@uowmail.edu.au (S. Peracchi), anatoly@uow.edu.au (A.B. Rosenfeld).

https://doi.org/10.1016/j.asr.2021.01.041
0273-1177/

sources: the Galactic Cosmic Rays (GCRs) constantly propagate in our solar system, the more sporadic, but even more intense Solar Particle Events (SPEs) which generate a flux of protons coming from solar explosions, and finally protons trapped by the geomagnetic field in the Van Allen Belts (Benton and Benton, 2001). The cocktail of protons coming from all sources ends up in a wide energy spectrum up to hundreds of GeV.

Currently, several Monte Carlo-based and other codes (Wilson et al., 2015, Wilson et al., 2004, Pinsky et al., 2001, Wilson et al., 1995) are used to simulate proton fluxes in space and to predict particles transport and interaction with spacecraft to assess dose and dose equivalent and consequently radiobiological effects on humans (Peracchi et al., 2019). In order to validate the simulated results, benchmarking experiments must be carried out. There are only a few radiation facilities in the world which can partially reproduce the radiation environment in space using high energy ion accelerators. Most of them only provide monoenergetic and unidirectional protons beams, which are not enough to mimic the real scenario in space (National Academies of Sciences Engineering and Medicine, 2018, Koziukov and Tuzhikova, 2015, Miller, 2003, Zeitlin et al., 2001, Benton et al., 2001, Kim et al., 2015). Moreover, space exploration is aiming to send humans to the Moon and to Mars for a longer period of time. The paramount need of knowing the effects related to astronauts' health and damage in space electronics deriving from such new and more dangerous radiation environments beforehand can be achieved only through ground-based radiation tests performed with whole energy spectra of protons to complement and validate the simulations. In fact, "In preparation for sending astronauts on long duration missions into space, it is necessary to simulate the same overall environment in ground-based facilities" (Norbury et al., 2016).

For many years, ground-based facilities approach the problem of reproducing the complex radiation scenario encountered in space. Some studies with multiple ion energies and angles have been successfully performed. Thanks to the enhancement of the technology at the NASA Space Radiation Laboratory, it is nowadays possible to switch beam energy and ion type in an order of 2 min to achieve a more realistic energy spectrum generated by the GCR simulator (Norbury et al., 2016, Simonsen et al., 2020). The Northeast Proton Therapy Center also offers radiation testing services using degraded proton beams (Cascio et al., 2004, Sisterson et al., 1999). Additionally, the isotropic nature of the radiation environment in space must be reproduced in a ground-based campaign, considering large angle irradiation as partially done in the experimental campaign performed at the Loma Linda University Proton Therapy Centre (Benton et al., 2001). However, it was repeatedly affirmed that the uncertainty associated with representing the GCR spectrum with discrete ion and energy beams, due also to constraints of current facilities, does influence the accuracy in evaluating the dose to astronauts (Slaba et al., 2016, Slaba et al., 2014). Many of these shortcomings in current ground radiation testing facilities for modeling of space radiation effects are continuously discussed at Workshops on Radiation Monitoring on the ISS (http://www.wrmiss.org/) and IEEE NSREC conferences (http://nsrec.com).

This paper aims to introduce a methodology to the scientific community that addresses the cited-above constraints, by describing how to program and use a treatment planning system (TPS) of a clinical accelerator to deliver a modulated fluence based on the intensity of a realistic spectrum previously simulated with GEANT4 or any other Monte Carlo code. This proposed methodology can potentially overcome the limitations of conducting tests with several mono-energetic beams delivered one at a time.

Particularly, in this work the methodology was applied to a portion of the proton field typical of Low Earth Orbit (LEO) environment in the available energy range from 70 to 230 MeV achievable with the clinical proton therapy accelerator at the Paul Scherrer Institute (PSI). Hence, results of microdosimetric characterization of proton fields with spectral properties typical of GCR, SPE, and Van Allen Belts protons delivered in a single experimental session with the clinical proton accelerator at PSI, controlled by a specially programmed TPS, are reported.

2. Materials and methods

2.1. Proton facility at PSI

In the '90 s, the Paul Scherrer Institute (PSI) was the first one in the world to develop a scanning gantry for proton therapy. Later PSI developed a second-generation Gantry 2, taking advantage of the experience gained from Gantry 1. It implements advanced magnetic scanning modes, which allow a significant reduction in the treatment time. Thus, it is possible to repeatedly irradiate a target with a one-side rotation from $-30°$ to $+ 180°$ in a reasonable time.

The accelerator used at PSI is a 250 MeV superconducting cyclotron, generating protons with a beam current extracted in a range from 0.05 to 850nA, which can be varied smoothly. An energy degrader, consisting of two sets of carbon wedges, moved mechanically very quickly in and out of the beam, allows changing the energy of the protons in a range of 70 to 230 MeV, within approximately 80 ms (Pedroni et al., 2011). In this experiment, the adopted beam current was in a range of 0.5 to 1nA, much lower than the typical current used for patients' treatments (200 – 400nA) with pencil beam scanning (PBS).

The vacuum of the beamline extends to the end of the nozzle reducing the distance in air from the vacuum window to isocenter down to 90 cm. The nozzle of the gantry, i.e. the proton beam exit foil, has a minimum required thickness to minimize the broadening of the protons pencil beam due to scattering effects and prevent neutron contam-

ination of the beam. For three main energies of interest, the sigma of the pencil beam width was: 5, 2.75, and 2.15 mm for 70, 150, 230 MeV, respectively, with a stable penumbral uncertainty of ± 0.35 mm (Pedroni et al., 2011). Within the nozzle, two plane-parallel ionization chambers measure the instantaneous intensity of the pencil beam, calibrated to the number of delivered protons per single delivered spot. Moreover, by selecting a particular field size of 5x5cm^2, and a spot spacing of 0.4 cm at the isocenter to deliver a uniform irradiation field, the number of spots per single layer can be calculated and consequently, the total number of protons delivered by the machine. Thus, the distribution of the protons density for each layer is expected to be homogeneous (Fig. 1).

2.2. Experimental set-up

In this study, a 3D sensitive volume microdosimeter fabricated on a silicon on insulator (SOI) wafer was used. The microdosimeter named "Mushroom" consists of a 20 × 20 matrix of cylindrical sensitive volumes (SVs) where the energy is deposited by the particle. Each SV has a planar n^+ core in the middle produced by ion implantation (planar technology and surrounded with a complete p^+ doped trench filled with polysilicon (Fig. 2a) which is forming a p-n junction. Each SV has dimensions of 18 μm diameter and 10 μm height. The microdosimeter was designed by the Centre for Medical Radiation Physics (CMRP), University of Wollongong, and fabricated at SINTEF MiNaLab, Oslo, and mounted on a 2 mm thick Dual-In-Line (DIL) package (James et al., 2019, Kok et al., 2020). Fig. 2 shows the SOI microdosimeter connected to the MicroPlus μ^+ probe, which has been tested successfully multiple times in heavy ions beams mimicking the heavy ions component of GCRs (Peracchi et al., 2020, James et al., 2019).

The advantage of microdosimetry is its capability of measuring the distribution of the stochastic energy deposition ε in a micron-sized SV, and from this calculate the lineal energy$y$, as the ratio between ε in a single event and the mean chord of the SV, which in our case was considered equal to the SV thickness (10 μm) of the SOI microdosimeter. The mean average chord of the cylindrical SV with

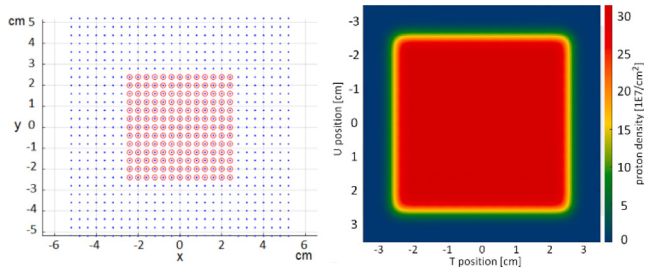

Fig. 1. Example of pencil beam pattern for a field size of 5x5cm^2 (left), and corresponding homogeneous proton fluence distribution delivered with of 5x10^7 protons/spot of Gaussian intensity distribution at 230 MeV (right).

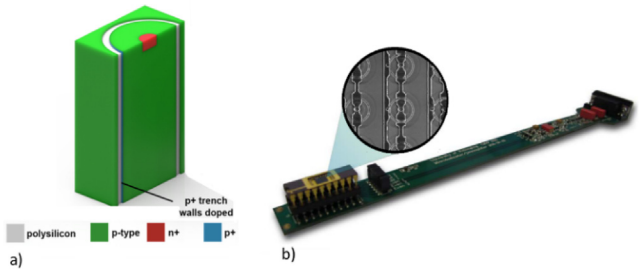

Fig. 2. a) The cylindrical sensitive volume (SV) of the "Mushroom" microdosimeter and b) the microdosimetric probe (μ+ probe), with the "Mushroom" microdosimeter connected at the left end. A zoomed-in Scanning Electron Microscope (SEM) image shows a top view of SVs array of the microdosimeter.

aspect ratio 2:1 is equal to the height of the SV that is approximately the case for mushroom SV with a diameter 18 μm and height 10 μm (Bolst et al., 2018). The microdosimetric spectra $yd(y)vsy$ expressed in logarithmic scale is derived using the frequency distribution of lineal energy $f(y)$, and corresponding to that the dose lineal energy distribution $d(y) = yf(y)$.Without a priori knowledge of a mixed radiation field in terms of particle type and energy, the microdosimetric measurements allow the evaluation of the average quality factor $\bar{Q}$of the radiation field, and the dose equivalent $Hp(10)$for astronauts' individual monitoring, as explained elsewhere (Peracchi et al., 2020).

The SOI microdosimeter is placed at the center of a PMMA cylindrical tube of inner diameter of 44 mm with a wall thickness of 10 mm to mimic isotropic conditions for any angle of the beam incidence. The PMMA cylinder has been chosen as an approximation of the human tissue to obtain the individual dose equivalent at 10 mm depth in the body ($Hp(10)$). Finally, a 75 μm aluminum foil was used to cover the PMMA phantom as a faraday cage in order to avoid the detection of radiofrequency noise in the detection electronics (Fig. 3b). The microdosimetric probe (MicroPlus) was installed in a freestanding position to allow a 180° rotation of the gantry around the SOI microdosimeter without interfering with the couch. The microdosimeter was placed at the isocenter of the gantry system (Fig. 3a). The gantry was programmed to deliver the same proton spectral field with 10° interval. In this paper, the response of the microdosimeter measured for gantry angles 0°, 90°, and 180° is presented.

2.3. Fluence modeling

Knowledge of the particle types, their energies and spectral fluence is extremely important for the prediction of biological effects on astronauts' health.

The GCR, SPE, and Van Allen protons spectra encountered at the ISS's altitude were partially reproduced using a custom treatment planning system at PSI and then delivered by the PSI clinical proton therapy control system (TCS). Since the protons per spot for each proton energy

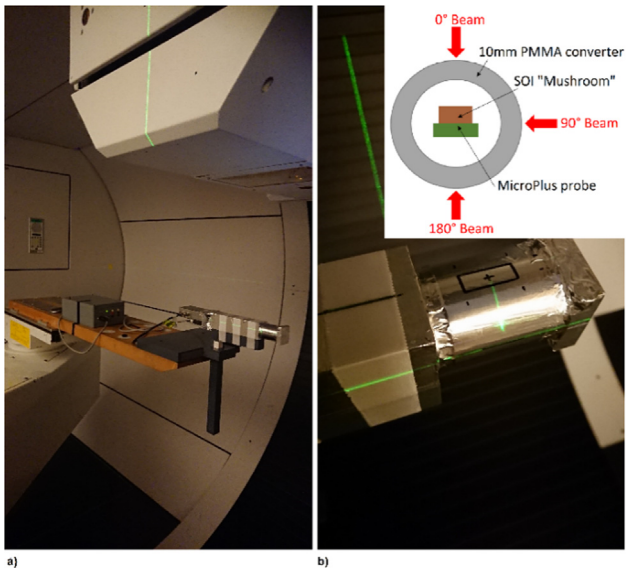

Fig. 3. a) Experimental set up inside the Gantry2 room; b) 10 mm PMMA cylindrical converter covered with aluminum foil hosting the SOI microdosimeter at the isocenter ("black cross" mark is where the SOI microdosimeter is located).

is an input to the TCS, it was possible to deliver the proton fluence of particular energies normalized to the corresponding spectrum of space radiation of interest. The proton fluence spectra of GCR, SPE, and Van Allen protons outside and inside the ISS Columbus for the LEO environment used in this study were previously simulated and investigated in the published work by our group (Peracchi et al., 2019). To briefly summarize: simulations of an isotropic proton fluence φ_{GEANT4} (protons cm^{-2} s^{-1} sr^{-1}) incident on the ISS/Columbus' module was done with GEANT4. A realistic geometry of the Columbus module was implemented based on specifications about its structure and shielding materials found in the literature (Destefanis et al., 2014, Silvestri et al., 2011). The output of the simulation was the fluence of the particles of the radiation field inside the Columbus habitat, including primary protons passing through the shielding wall of the spacecraft and, eventually, secondary particles produced by interaction with the ISS wall's materials. More details about the simulation model can be found in (Peracchi et al., 2019). The calculated proton fluences in the Columbus habitat in the range 70 to 230 MeV with a 1 MeV energy steps (see the yellow area in Fig. 4) were taken as an input to the TPS, due to limits of the available protons energy achievable with the used medical accelerator. Even though it represents a narrowed part of a realistic full spectrum, referring to Fig. 4 for example, this energy range represents the 9, 52, and 63% of the entire fluence spectra of GCR, SPE, and Van Allen Belts protons inside the ISS, respectively.

Next, the protons fluence for each bin along the spectrum was calculated by referring to the planned fluence of 70 MeV protons and scaled to the space proton fluence.

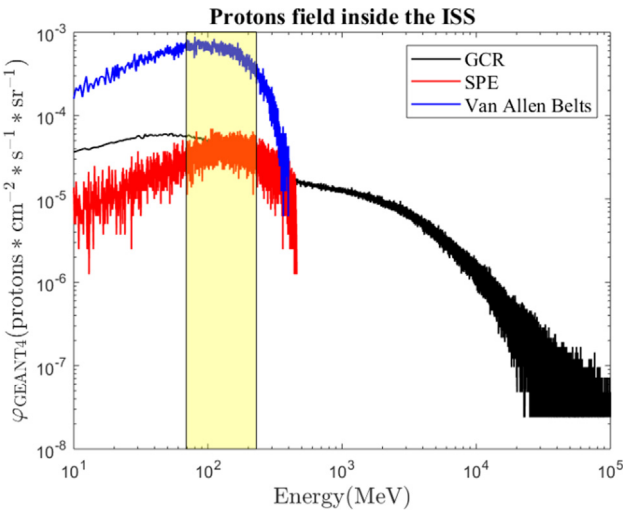

Fig. 4. Example of protons fluences inside the ISS simulated with GEANT4 in previous work (Peracchi et al., 2019); fluxes include both primary and secondary protons generated by nuclear interaction with shielding wall. The yellow area highlights the range of energy (70 to 230 MeV) used in this study. (For interpretation of the references to colour in this figure legend, the reader is referred to the web version of this article.)

The TPS associates a minimum value of protons per spot delivered $(\#p/s)_{min}$ at the energy layer with the lowest simulated fluence to guarantee a minimum acceptable statistic and consequently rescales the value $(\#p/s)_i$ for all remaining bin energies E_i. Additionally, to avoid pileup, the current is lowered to the level the system could withstand. This value is the one expected to be delivered at the isocenter in free air geometry, where the SOI microdosimeter was placed. Knowing the field size A of 5x5cm^2, equivalent to the area of a single-energy layer i, and the total number of spots in one layer $(\#s)$, 13x13 spots, the fluence expected to be delivered by the TPS φ_{TPS-i} (protons cm^{-2}) for each energy layer i was calculated as follows:

$$\varphi_{TPS-i} = \frac{(\#p/s)_i * \#s}{A} \quad (1)$$

Finally, for each irradiation, the two ionization chambers in the nozzle record the actual number of protons delivered per spot by the TPS ($\varphi_{TPS-expected}$), to account for any uncertainties in the beam current delivered. Such uncertainties are larger at the low currents used in this experiment, while are almost negligible at the higher currents used clinically. By using the formula in Equation (1), the actual fluence delivered by the TPS at the isocenter ($\varphi_{TPS-delivered}$) was calculated for each irradiation and angle.

2.4. Dose evaluation

As mentioned in the previous section, the SOI microdosimeter set-up was implemented to evaluate the dose equivalent $Hp(10)$ at 10 mm depth in the body of an astronaut. The theoretical absorbed dose D_{TPS-i}(Gy), at the isocenter planned by the TPS and delivered for protons

with energy E_i, was calculated as at the entrance of a hypothetical water phantom by the following formula:

$$D_{TPS-i} = \frac{\varphi_{TPS-i} * LET_i}{\rho} \quad (2)$$

where $\rho = 1\ \mathrm{g\ cm^{-3}}$ is the density of water and the LET_i for protons in water was calculated with SRIM for each energy value $E_i$from 70 MeV to 230 MeV.

The total entrance absorbed dose in water delivered in any particular irradiation is a sum of contributions for each energy in a full spectrum:

$$D_{TPS} = \sum_{i=70MeV}^{230MeV} D_{TPS-i} \quad (3)$$

By analyzing the microdosimetric spectra $yd(y)$ *vs* y measured by the SOI microdosimeter, the calculation of the average quality factor $\bar{Q}$ of the protons field is performed, providing the formula stated by the International Commission on Radiological Protection (ICRP) Publication 60 (International Commission on Radiological Protection, 1991). Therefore, the value of $Hp(10)$ is calculated based on the measured absorbed dose in silicon D_{Si}:

$$Hp(10) = (D_{Si} * 0.80) * \bar{Q} = D_{TE} * \bar{Q} \quad (4)$$

where 0.8 is the tissue-equivalent factor for conversion of absorbed dose in silicon to tissueD_{TE} obtained as the average of proton mass stopping power ratio silicon to water in a proton energy range 70 to 230 MeV.

Finally, the $Hp(10)$ measured by the SOI microdosimeter is normalized by the corresponding value of entrance-absorbed dose delivered in water by the gantry for each irradiation. Even though the dose equivalent is not a protection quantity adopted for radiation protection in space, it is still considered as important supplementary information, providing an additional quantity that can be useful to quantify biologically relevant hazard of the reference field (International commission on radiation units and measurements the International commission on radiological protection, 2017, Slaba et al., 2016, Benton et al., 2001).

3. Results

3.1. Modeling of the fluence and dose

Fig. 5 shows the comparison of expected spectral fluence for GCR, SPE, and Van Allen Belts (or trapped) protons outside and inside the ISS obtained with GEANT4 (Peracchi et al., 2019) with the reproduced proton spectra obtained using the custom TPS and delivered at gantry angle 0°, considering a minimum number of protons per spot $(\#p/s)_{min} = 10^5$. It can be seen that they match reasonably well. The TPS planed and delivered spectral fluences match the expected modeled with GEANT4 fluence with a relative standard deviation σ between 3% and 5%. The uncertainty in fluence delivery correlates with the beam current: particularly, the lower the current, the higher the difference between delivered fluence and planned by TPS. Consistent results were obtained also for the 90° and 180° irradiations.

Fig. 6 shows spectral absorbed doses for each energy simulated by GEANT4, modeled and delivered by the TPS at the isocenter in both scenarios, outside and inside the ISS. As expected, the absorbed dose is characterized by the same uncertainty associated with the corresponding fluence in Fig. 5, particularly σ is in a range of 3 to 5%. The same uncertainty was observed for 90° and 180° irradiations but not presented here.

3.2. Microdosimetric spectra measured by the SOI "Mushroom"

The response of the microdosimeter was studied using a delivered proton spectral fluence mimicking the ISS radiation environment. Fig. 7 shows microdosimetric spectra measured by the SOI "Mushroom" microdosimeter during the delivery of GCR, SPE, and trapped proton spectral fluences discussed in the previous section, by a medical accelerator. Fig. 7a shows the microdosimetric spectra obtained at 0°, 90°, and 180° for GCR, SPE, and trapped protons outside and inside the ISS. In the case of GCR and SPE proton spectral fluences, the microdosimetric spectra for proton beam incident at 0° and 180° have essential partial contribution events with lineal energies below 10 keV/μm (all presented lineal energies are related to tissue). For 90° beam incidence, the microdosimetric spectrum was shifted to higher lineal energies above 10 keV/μm in both cases due to charge deposited in two or more "Mushroom" SVs which are read out as a single event.

For GCR outside the ISS, no essential difference between microdosimetric spectra measured at 0° and 180° was observed. It is due to the fact that the majority of these protons have energy above 160 MeV and not modified essentially by transmission through 2 mm thick plastic of the DIL package. Inside the ISS, the proton spectrum is with descending partial contribution of higher energy protons that led to a slightly higher proportion of lower lineal energy events for 0° beam incidence in comparison to outside ISS microdosimetric spectra. It is caused by fewer events in a higher lineal energy tail due to inelastic reactions occurring in silicon and PMMA induced by high energy protons (e.g. Si(p,α), Si(p,p)) generating alpha particles and recoil Si atoms. Even the single event with $y > 100$ keV/μm will lead to a visible change of the lower y component of microdosimetric spectra. For 180° beam incidence, this effect is more pronounced because of additionally absorption of high LET particles generated in PMMA by DIL package and due to relative visible contribution of degradation energy of low energy protons (70 MeV) by DIL package, after they lost energy in 10 mm of PMMA. Both mentioned reasons are reflected in much higher partial contribution to microdosimetric spectra of events with $y < 10$ keV/μm and slightly widening of this part of the microdosimetric spectrum in comparison

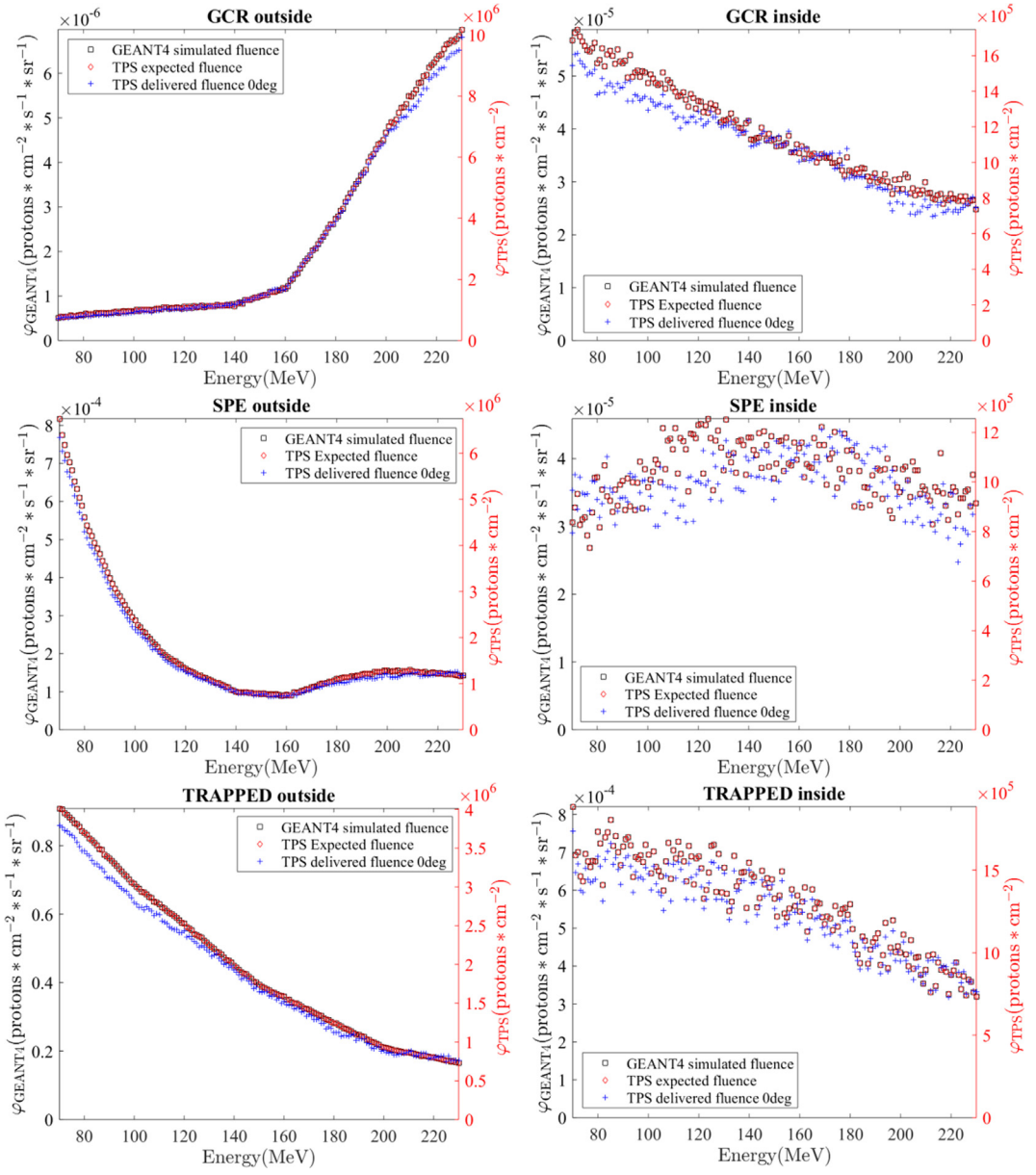

Fig. 5. GCR, SPE, and trapped protons spectral fluence delivered by the gantry at the isocenter (blue +), compared with the fluence modelled with the TPS (red ◊) and GEANT4 (black □) simulation. The TPS red lines and GEANT4 black lines match perfectly as expected. Two scenarios were considered: spectra outside the ISS/Columbus module and inside it after protons propagating through the shielding of the spacecraft. (For interpretation of the references to colour in this figure legend, the reader is referred to the web version of this article.)

with outside of ISS. The effect of softening of the proton spectra inside the ISS is also reflected in a slight shift of microdosimetric spectra to higher y for 90° beam incidence in comparison with corresponding microdosimetric spectra outside ISS.

For the SPE spectrum outside the ISS, the essential partial contribution of lower energy protons makes the microdosimetric spectrum wider and skewed to higher lineal energies in comparison to GCR microdosimetry spectra for both 0° and180°. The identity of both microdosimetric spectra is explained with the absence of single high lineal energy events due to much lower partial contribution of higher energy protons in SPE spectrum outside the ISS. The inside proton spectrum is much more uniformly distributed with an equal partial contribution of lower and higher energy protons that is reflected in higher partial contribution of lower lineal energy events for 0° incidence angle in comparison to microdosimetric spectra outside the ISS (see explanation above). It is also confirmed by a shift of 90° microdosimetric spectra to lower lineal energies in comparison with corresponding microdosimetric spectra outside the ISS.

For trapped protons, the microdosimetric spectra for 0° and 90° beam incidence are identical for the inside and outside ISS scenarios due to similar proton spectral fluence (see Fig. 5). For all three protons spectra at 90°, the micro-

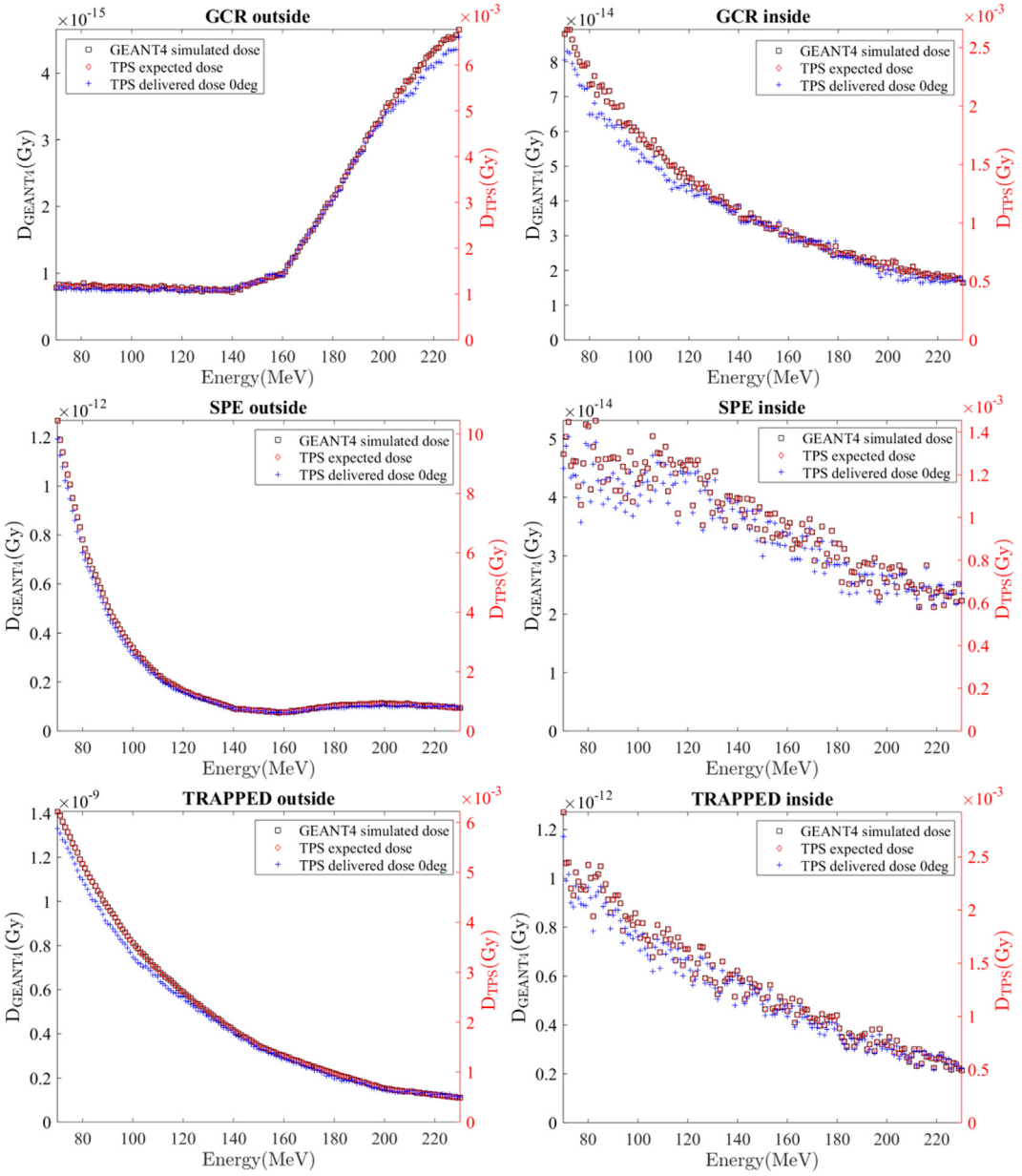

Fig. 6. Spectral absorbed dose delivered by the gantry at the entrance to water at isocenter (blue +), compared with the absorbed dose modeled with the TPS (red ◊) and based on GEANT4 (black □) simulation, for GCR, SPE, and trapped protons beams, outside and inside the ISS/Columbus module. (For interpretation of the references to colour in this figure legend, the reader is referred to the web version of this article.)

dosimetric spectra shifted to higher lineal energy due to enhanced energy deposition by protons passing multiple SVs in the detector that is electrically connected to the same readout bus. In fact, values of $Hp(10)$ calculated at 90° are at least a factor 2 higher than doses measured at 0° and 180°, considering the same dose delivered by the clinical machine (see Table 1). However, the probability of such events in the cosmic isotropic field is extremely low due to the small size of the "Mushroom" SV and associate to that acceptance solid angle for such events. To mitigate such events, the "Mushroom" design has odd and even linear arrays of SVs connected to different readout preamplifiers.

Table 1 shows the average values for the quality factors $\bar{Q}$ derived based on convolution of measured microdosimetric spectra and ICRU 60 recommended $Q(LET)$ (International Commission on Radiological Protection, 1991). Measured $\bar{Q}$ values of this study were compared with predicted values based on GEANT4 modelling of the SOI "Mushroom" microdosimeter's response inside the ISS for proton spectral fluence extended up to 10^5 MeV as realistic GCR, SPE, and trapped proton spectra. GEANT4 predicted values 1.30, 1.31 and 1.41 for GCR, SPE and trapped protons respectively (Peracchi et al., 2019), are a bit lower than values measured by the SOI in this study, but still considered close to the interval error. Particularly values obtained for SPE (1.67) and trapped protons (1.48)

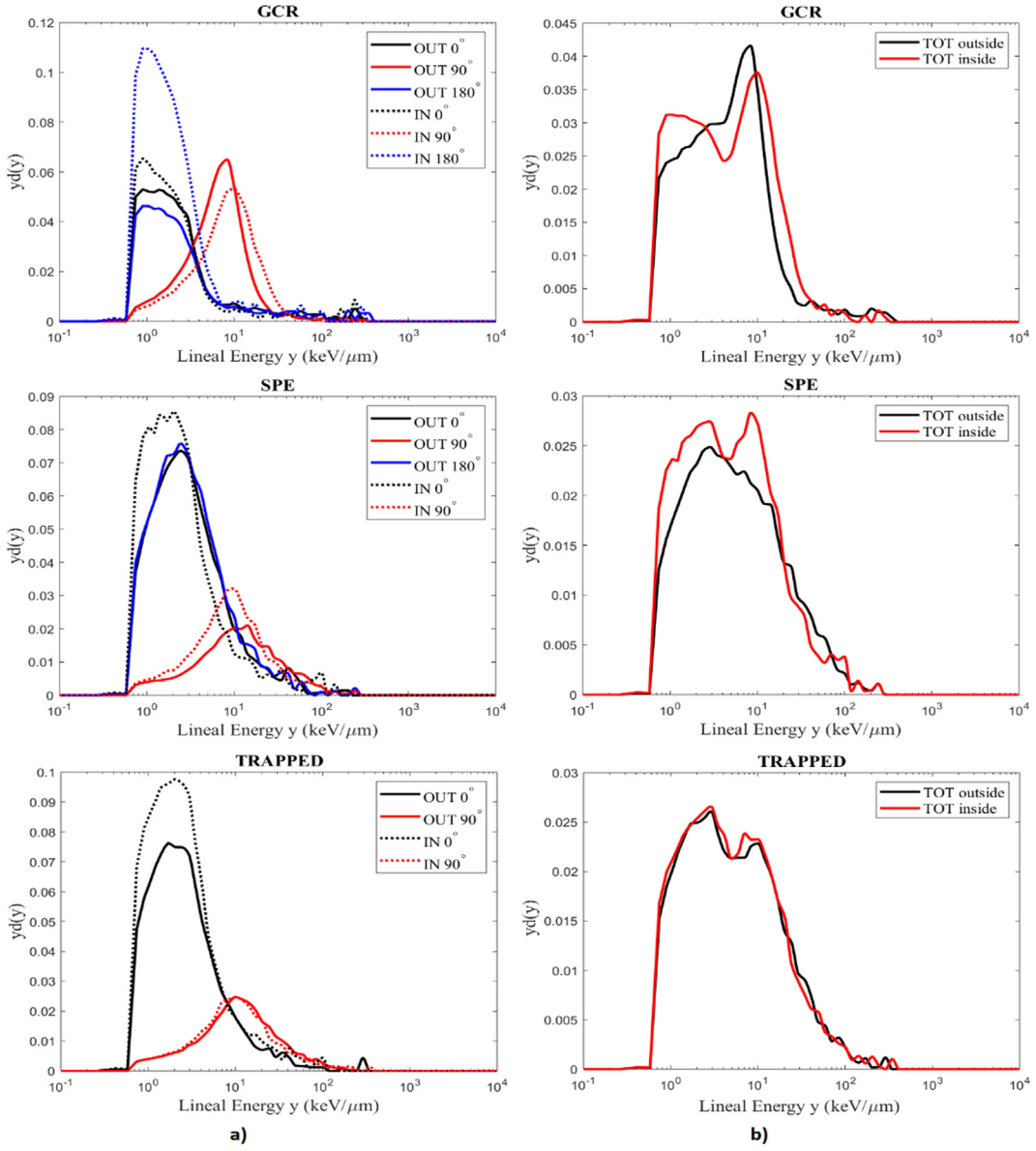

Fig. 7. a) Microdosimetric spectra measured by the SOI microdosimeter during 0°, 90°, and 180° irradiations, modeling the proton fluence outside the ISS/Columbus (solid lines) and inside it (dashed lines). b) Microdosimetric spectra resulting from an isotropic irradiation over 180°.

and GCR scenario (1.89) under 0°beam can be explained essentially by the fact that the proton spectral fluence considered in this study is just limited to an energy range of 70 ÷ 230 MeV. For SPE and trapped most of proton spectral fluence is below 230 MeV protons and well reflected in our experiment, but still the contribution of protons with energy up to 500 MeV is not considered. Similar for GCR protons up to 100 GeV: the high energy proton component, while with low LET, provides high energy delta electrons that produce a not negligible contribution to absorbed dose and microdosimetric spectra for $y < 0.4$ keV/μm, which is not counted in present experiments. The convolution of the low lineal energy tail of microdosimetric spectra with $Q(LET)$ will lead to a reduction of $\bar{Q}$ which explains the observed difference. Additionally, this comparison demonstrates that the performance of the SOI "Mushroom" microdosimeter is matching to theoretical expectations.

In Fig. 7b, another series of results is presented, by means of the microdosimetric spectra resulting from an approximated isotropic irradiation over 180°. The total spectra were obtained by merging the original MCA files for the same delivered fluence from the three irradiations at 0°, 90°, and 180° and performing the usual analysis as explained above. These results show a realistic approximation of how the microdosimetric spectra would look like in case of isotropic irradiation over 180°. Unfortunately, irradiations at 180° with SPE and trapped inside spectra and 180° trapped outside spectrum were not available, hence the missing inside microdosimetric spectra at 180° were assumed to be equal to the inside microdosimetric spectra obtained at 0°. Similarly, for the missing trapped protons

Table 1
Values of dose calculated based on microdosimetric spectra analysis compared to dose delivered by tps.

Beam	Angle	$\bar{Q}$	D_{TPS}(Gy)	Hp(10)(Sv/Gy)
GCR out	0°	2.02 ± 0.16	0.40	0.33 ± 0.01
	90°	1.73 ± 0.06	0.40	0.83 ± 0.01
	180°	2.12 ± 0.17	0.39	0.36 ± 0.01
GCR in	0°	1.89 ± 0.22	0.18	0.40 ± 0.01
	90°	2.04 ± 0.06	0.18	1.07 ± 0.01
	180°	1.48 ± 0.13	0.18	0.32 ± 0.01
SPE out	0°	1.59 ± 0.08	0.29	0.45 ± 0.01
	90°	4.25 ± 0.15	0.29	1.82 ± 0.02
	180°	1.50 ± 0.08	0.29	0.36 ± 0.01
SPE in	0°	1.67 ± 0.14	0.15	0.43 ± 0.01
	90°	3.16 ± 0.15	0.15	1.68 ± 0.02
Trap out	0°	1.46 ± 0.08	0.32	0.43 ± 0.01
	90°	3.91 ± 0.12	0.32	1.98 ± 0.02
Trap in	0°	1.48 ± 0.09	0.20	0.41 ± 0.01
	90°	3.61 ± 0.15	0.20	1.90 ± 0.02
GCR out	TOT	1.87 ± 0.06	1.19	0.50 ± 0.02
GCR in		1.88 ± 0.07	0.54	0.59 ± 0.01
SPE out		2.77 ± 0.07	0.88	0.88 ± 0.02
SPE in		2.43 ± 0.09	0.45	0.85 ± 0.01
Trap out		2.60 ± 0.06	0.97	0.94 ± 0.02
Trap in		2.53 ± 0.08	0.59	0.91 ± 0.01

microdosimetric spectrum at 180° outside, considered the same as the one measured at 0° outside the ISS. The assumption was made based on the similarity observable in Fig. 7a, confirmed by values of $\bar{Q}$ and $Hp(10)$ in Table 1.

4. Conclusions

This paper introduces a methodology to model the proton spectral fluence typically encountered in space using a programmed treatment planning system of a proton therapy accelerator. The study was conducted at the proton therapy centre Paul Scherrer Institue, where the fractional proton spectra of GCR, SPE, and Van Allen Belts in an energy range from 70 to 230 MeV were delivered by a pencil scanning beam. These spectra used as an example of input were obtained by ad-hoc GEANT4 simulations of the radiation environment at the ISS's altitude (Peracchi et al., 2019).

The number of protons per each spot and energy was provided by the TPS to replicate the particular proton spectral fluence. A 5x5 cm^2 field of uniform proton fluence was delivered at the isocenter, where the microdosimeter was placed. Two ionization chambers placed at the window exit of the nozzle detected and controlled the actual fluence delivered independently on possible the beam current fluctuations to guarantee the best match with what expected from the TPS. This new methodology allows also the irradiation of electronic components or biological objects with a LET programed proton spectra that is important for SEU studies and radiobiological models verification. The advantage of delivering a modulated fluence based on the intensity of a realistic spectrum allows to skip the constant change in the beam set up to switch energy, gaining time and reducing the uncertainty.

It is the first time that the SOI "Mushroom" microdosimeter was irradiated in a cylindrical PMMA phantom with a realistic space partial proton spectral fluence isotropic field and the microdosimetric spectra were obtained. The quality factor $\bar{Q}$ and the personal dose equivalent $Hp(10)$ per unit of absorbed proton entrance dose in water at the isocenter were evaluated for radiation protection purposes, in two scenarios: astronauts outside and inside the ISS/Columbus.

Results on delivered spectral fluence and the quality factor $\bar{Q}$ are consistent with previously simulated results for this microdosimeter using Geant4 in the same proton spectral fields (Peracchi et al., 2019) confirming the accuracy of the implemented methodology to deliver any spectrum of interest simulated with Monte Carlo model. This study with spectral proton fluence and previous study with heavier ions in (Peracchi et al., 2020) demonstrated that SOI microdosimeter can accurately measure LET(Si) in a wide range (0.5 ÷ 5000) keV/μm and can be useful for SEU prediction additionally to astronauts radiation protection.

Approach and gained experience with proton medical accelerator for proton space field reproducing will be translated to HIMAC (Japan) for modeling of GCR ion spectral fluence of He, C, O and Fe following progress in the development of multi-ion therapy delivery and TPS for that (Inaniwa et al., 2020).

Declaration of Competing Interest

The authors declare that they have no known competing financial interests or personal relationships that could have appeared to influence the work reported in this paper.

Acknowledgment

We would like to thank the team of researchers from the Paul Scherrer Institute, for the great help provided during the run of the proton therapy clinical machine. The custom TPS used for our specific delivery was based on tools developed at PSI by G. Klimpki and S. Psoroulas.

We would like to thank the Australian Research Council (ARC) for supporting this research with a Discovery Project Grant "Development of radiation detectors to better understand ion interactions" (DP 170102273) and the European Space Agency (ESA) with the grant "Tissue equivalent crew dosimeter based on novel 3D Si processing" (Contract No. 4000112670/14/NL/HK).

References

Benton, E.R., Benton, E.V., 2001. Space radiation dosimetry in LEO and beyond. Nucl. Instruments Meth. Phys. Res. B 184, 255–294.

Benton, E. R., Benton, E. V. & Frank, A. L. 2001. Characterization of the radiation shielding properties of U.S. and Russian EVA suits. In:

REPORTS, O. O. S. T. I. T. (ed.). Lawrence Berkeley National Laboratory,.

Bolst, D., Guatelli, S., Tran, L.T., Rosenfeld, A.B., 2018. Optimisation of the design of SOI microdosimeters for hadron therapy quality assurance. Phys. Med. Biol. 63 215007.

CASCIO, E. W., SISTERSON, J. A., GOTTSCHALK, B. & SARKAR, S. Measurements of the energy spectrum of degraded proton beams at NPTC. IEEE Radiation Effects Data Workshop (IEEE Cat. No.04TH8774), 2004. 151-155.

DESTEFANIS, R., AMERIO, E., BRICCARELLO, M., BELLUCO, M., FARAUD, M., TRACINO, E. & LOBASCIO, C. Space environment characterisation of Kevlar®: good for bullets, debris and radiation too. SPACEEC, 2014. Thales Alenia Space Italia S.p.A and Sofiter System Engineering, 80-113.

INANIWA, T., SUZUKI, M., HYUN LEE, S., MIZUSHIMA, K., IWATA, Y., KANEMATSU, N. & SHIRAI, T. 2020. Experimental validation of stochastic microdosimetric kinetic model for multi-ion therapy treatment planning with helium-, carbon-, oxygen-, and neon-ion beams. Physics in Medicine & Biology, 65, 045005

INTERNATIONAL COMMISSION ON RADIATION UNITS AND MEASUREMENTS & THE INTERNATIONAL COMMISSION ON RADIOLOGICAL PROTECTION 2017. Operational Quantities for External Radiation Exposure

INTERNATIONAL COMMISSION ON RADIOLOGICAL PROTECTION 1991. ICRP Publication 60: 1990 Recommendations of the International Commission on Radiological Protection. In: 1-3 (ed.) Annual of the ICRP

James, B., Tran, L.T., Bolst, D., Peracchi, S., Davis, J.A., Prokopovich, D.A., Guatelli, S., Petasecca, M., Lerch, M., Povoli, M., Kok, A., Goethem, M.-J., Nancarrow, M., Matsufuji, N., Jackson, M., Rosenfeld, A.B., 2019. SOI Thin Microdosimeters for High LET Single Event Upset Studies in Fe, O, Xe and Cocktail Ion Beam Fields. IEEE Trans. Nucl. Sci. 67, 146–153.

Kim, M.-H.Y., Rusek, A., Cucinotta, F.A., 2015. Issues for Simulation of Galactic Cosmic Ray Exposures for Radiobiological Research at Ground-Based Accelerators. Front. Oncol. 5.

KOK, A., POVOLI, M., SUMMANWAR, A., TRAN, L. T., PETASECCA, M., LERCH, M. L. F., BOLST, D., GUATELLI, S. & ROSENFELD, A. B. 2020. Fabrication and First Characterisation of Silicon-based Full 3D Microdosimeters. IEEE Transactions on Nuclear Science, 1-1

KOZIUKOV, A., TUZHIKOVA, I., PELLISH J, CHUBUNOV, P., PAILLET, P., ECOFFET, R., ANASHIN, V., BARBERO, S. M., HÖFFGEN, S. K., BERGER, G. & GUERRERO, H. Compendium of international irradiation test facilities. RADECS, 2015 Moscow, Russia.

MILLER, J. 2003. Proton and heavy ion acceleration facilities for space radiation research. Gravitational and space biology bulletin: publication of the American Society for Gravitational and Space Biology, 16, 19-36

NATIONAL ACADEMIES OF SCIENCES ENGINEERING AND MEDICINE 2018. Testing at the Speed of Light: The State of U.S. Electronic Parts Space Radiation Testing Infrastructure. In: THE NATIONAL ACADEMIES PRESS (ed.). Washington.

NORBURY, J. W., SCHIMMERLING, W., SLABA, T. C., AZZAM, E. I., BADAVI, F. F., BAIOCCO, G., BENTON, E., BINDI, V., BLAKELY, E. A., BLATTNIG, S. R., BOOTHMAN, D. A., BORAK, T. B., BRITTEN, R. A., CURTIS, S., DINGFELDER, M., DURANTE, M., DYNAN, W. S., EISCH, A. J., ROBIN ELGART, S., GOODHEAD, D. T., GUIDA, P. M., HEILBRONN, L. H., HELLWEG, C. E., HUFF, J. L., KRONENBERG, A., LA TESSA, C., LOWENSTEIN, D. I., MILLER, J., MORITA, T., NARICI, L., NELSON, G. A., NORMAN, R. B., OTTOLENGHI, A., PATEL, Z. S., REITZ, G., RUSEK, A., SCHREURS, A. S., SCOTT-CARNELL, L. A., SEMONES, E., SHAY, J. W., SHURSHAKOV, V. A., SIHVER, L., SIMONSEN, L. C., STORY, M. D., TURKER, M. S., UCHIHORI, Y., WILLIAMS, J. & ZEITLIN, C. J. 2016. Galactic cosmic ray simulation at the NASA Space Radiation Laboratory. Life Sci Space Res (Amst), 8, 38-51

Pedroni, E., Meer, D., Bula, C., Safai, S., Zenklusen, S., 2011. Pencil beam characteristics of the next-generation proton scanning gantry of PSI: design issues and initial commissioning results. European Phys. J. Plus 126, 1–27.

Peracchi, S., Tran, L.T., James, B., Bolst, D., Prokopovich, D.A., Davis, J.A., Guatelli, S., Petasecca, M., Lerch, M.L.F., Matsufuji, N., Kok, A., Povoli, M., Jackson, M., Rosenfeld, A.B., 2020. A solid-state microdosimeter for dose and radiation quality monitoring for astronauts in space. IEEE Trans. Nucl. Sci. 67, 169–174.

Peracchi, S., Vohradsky, J., Guatelli, S., Bolst, D., Tran, L.T., Prokopovich, D.A., Rosenfeld, A.B., 2019. Modelling of the Silicon-On-Insulator microdosimeter response within the International Space Station for astronauts' radiation protection. Radiat. Meas. 128.

Pinsky, L., Carminati, F., Ferrari, A., 2001. Simulation of Space Shuttle neutron measurements with FLUKA. Radiat. Meas. 33, 335–339.

Silvestri, M., Tracino, E., Briccarello, M., Belluco, M., Destefanis, R., Lobascio, C., Durante, M., Santin, G., Schrimpf, R.D., 2011. Impact of Spacecraft-Shell Composition on 1 GeV/Nucleon 56Fe Ion-Fragmentation and Dose Reduction. IEEE Trans. Nucl. Sci. 58, 3126–3133.

Simonsen, L.C., Slaba, T.C., Guida, P., Rusek, A., 2020. NASA's first ground-based Galactic Cosmic Ray Simulator: Enabling a new era in space radiobiology research. PLoS Biol. 18 e3000669.

SISTERSON, J. M., FLANZ, J. B. & BURNS, J. E. A new proton irradiation facility at the Northeast Proton Therapy Center. 1999 IEEE Radiation Effects Data Workshop. Workshop Record. Held in conjunction with IEEE Nuclear and Space Radiation Effects Conference, 12-16 July 1999 1999. 123-127.

Slaba, T.C., Blattnig, S.R., Norbury, J.W., Rusek, A., la Tessa, C., 2016. Reference field specification and preliminary beam selection strategy for accelerator-based GCR simulation. Life Sci. Space Res. (Amst) 8, 52–67.

Slaba, T.C., Xu, X., Blattnig, S.R., Norman, R.B., 2014. GCR environmental models III: GCR model validation and propagated uncertainties in effective dose. Space Weather 12, 217–224.

Wilson, J., Badavi, F., Cucinotta, F., Shinn, J., Badhwar, G., Silberberg, R., Tsao, C., Townsend, L., Tripathi, R., 1995. HZETRN: Description of a Free-Space Ion and Nucleon Transport and Shielding Computer Program. NASA STI/Recon Tech. Rep. N, 95.

Wilson, J.W., Slaba, T.C., Badavi, F.F., Reddell, B.D., Bahadori, A.A., 2015. 3DHZETRN: Shielded ICRU spherical phantom. Life Sci. Space Res. (Amst) 4, 46–61.

Wilson, J.W., Tripathi, R.K., Qualls, G.D., Cucinotta, F.A., Prael, R.E., Norbury, J.W., Heinbockel, J.H., Tweed, J., 2004. A space radiation transport method development. Adv. Space Res. 34, 1319–1327.

ZEITLIN, C., HEILBRONN, L. & MILLER, J. 2001. Radiation tests of the extravehicular mobility unit space suit for the international space station using energetic protons.